# Extreme summer weather in northern mid-latitudes linked to a vanishing cryosphere

Qiuhong Tang[1]*, Xuejun Zhang[1,2] and Jennifer A. Francis[3]

The past decade has seen an exceptional number of unprecedented summer extreme weather events[1-4] in northern mid-latitudes, along with record declines in both summer Arctic sea ice[5,6] and snow cover on high-latitude land[7]. The underlying mechanisms that link the shrinking cryosphere with summer extreme weather, however, remain unclear[8-12]. Here, we combine satellite observations of early summer snow cover and summer sea-ice extent[13] with atmospheric reanalysis data[14] to demonstrate associations between summer weather patterns in mid-latitudes and losses of snow and sea ice. Results suggest that the atmospheric circulation responds differently to changes in the ice and snow extents, with a stronger response to sea-ice loss, even though its reduction is half as large as that for the snow cover. Atmospheric changes associated with the combined snow/ice reductions reveal widespread upper-level height increases, weaker upper-level zonal winds at high latitudes, a more amplified upper-level pattern, and a general northward shift in the jet stream. More frequent extreme summer heat events over mid-latitude continents are linked with reduced sea ice and snow through these circulation changes.

Since the 1980s, Arctic sea ice extent (SIE) has declined at a rate of about 8% per decade during September[5], reaching a new record minimum in 2012. The area of summer sea-ice loss would cover over 40% of the contiguous United States[6]. Snow-cover extent (SCE) on high-latitude, Northern Hemisphere land areas has also diminished during early summer. The rate of SCE loss during June from 1979 to 2011 of 17.8% per decade is even faster than the loss rate of Arctic SIE (ref. 7). Along with these Arctic changes, a variety of extreme weather events have occurred during recent summers around the Northern Hemisphere: heat waves and droughts in the US (ref. 1) and parts of Europe (ref. 2 and references therein), generally cool wet summers with record rains and floods in the UK (ref. 3), and devastating rainfall extremes in East Asia[4], to mention just a few. Anthropogenic global warming is believed to contribute to the increasing number of extreme weather events[1,2] as well as to the accelerating loss of ice and snow in the Arctic[5,7]. The mechanisms that may relate the melting Arctic with extreme summer weather events, however, remain unclear, particularly in the context of Arctic temperature amplification[15,16], which also participates in strong feedbacks involving sea-ice loss[17,18].

Previous studies have reported statistical associations and feedbacks between large-scale atmospheric circulation changes and Arctic sea-ice loss (ref. 19 and references therein). The notion of changes in atmospheric circulation being linked with the recent extreme weather events in winter has also been suggested[12,20,21]. Atmospheric circulation patterns in northern mid-latitudes have been shifting in summer[9,22] as well, accompanied by an increasing
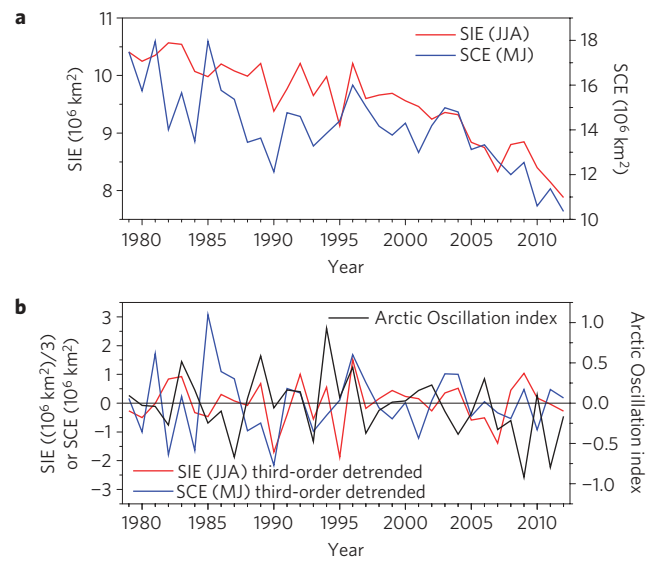
Figure 1 | SIE, SCE and Arctic Oscillation indices. a, Summer (JJA) Arctic SIE and early summer (May and June) Northern Hemisphere SCE. **b**, The third-order detrended summer SIE and early summer SCE indices (Methods) as well as the summer Arctic Oscillation index. Data span 1979–2012.

prevalence of extreme weather events in northern continents[1,2]. It has been suggested that the weakening poleward temperature gradient due to Arctic amplification is contributing to a slower progression of Rossby waves in upper-level flows, which in turn leads to more persistent weather conditions that favour extreme events in Northern Hemisphere mid-latitudes[10]. This leads to suspicion that the decline in SCE on high-latitude land during May and June may play a role by allowing the underlying soil to dry out and warm earlier[10], and therefore contribute to summer drought and heat waves in Europe[8] and North America, as well as to changes in the subarctic summer climate[11].

In this study we use atmospheric fields from reanalyses to extend this body of research by investigating the response of summer circulation patterns to losses of early summer snow cover and summer sea ice, and the relationship between those changes and extreme heat events over Northern Hemisphere continents.

Observed losses of summer (June, July and August; JJA) Arctic SIE and early summer (May and June) SCE on Northern Hemisphere land during 1979–2012 are shown in Fig. 1. The change in SCE from the 1980s to the 2000s is approximately double the area of sea-ice loss (3 million km² versus 1.5 million km²). The summer

[1]Institute of Geographic Sciences and Natural Resources Research, Chinese Academy of Sciences, Beijing 100101, China, [2]University of Chinese Academy of Sciences, Beijing 100049, China, [3]Institute of Marine and Coastal Sciences, Rutgers University, New Brunswick, New Jersey 08901, USA.
*e-mail: tangqh@igsnrr.ac.cn

1
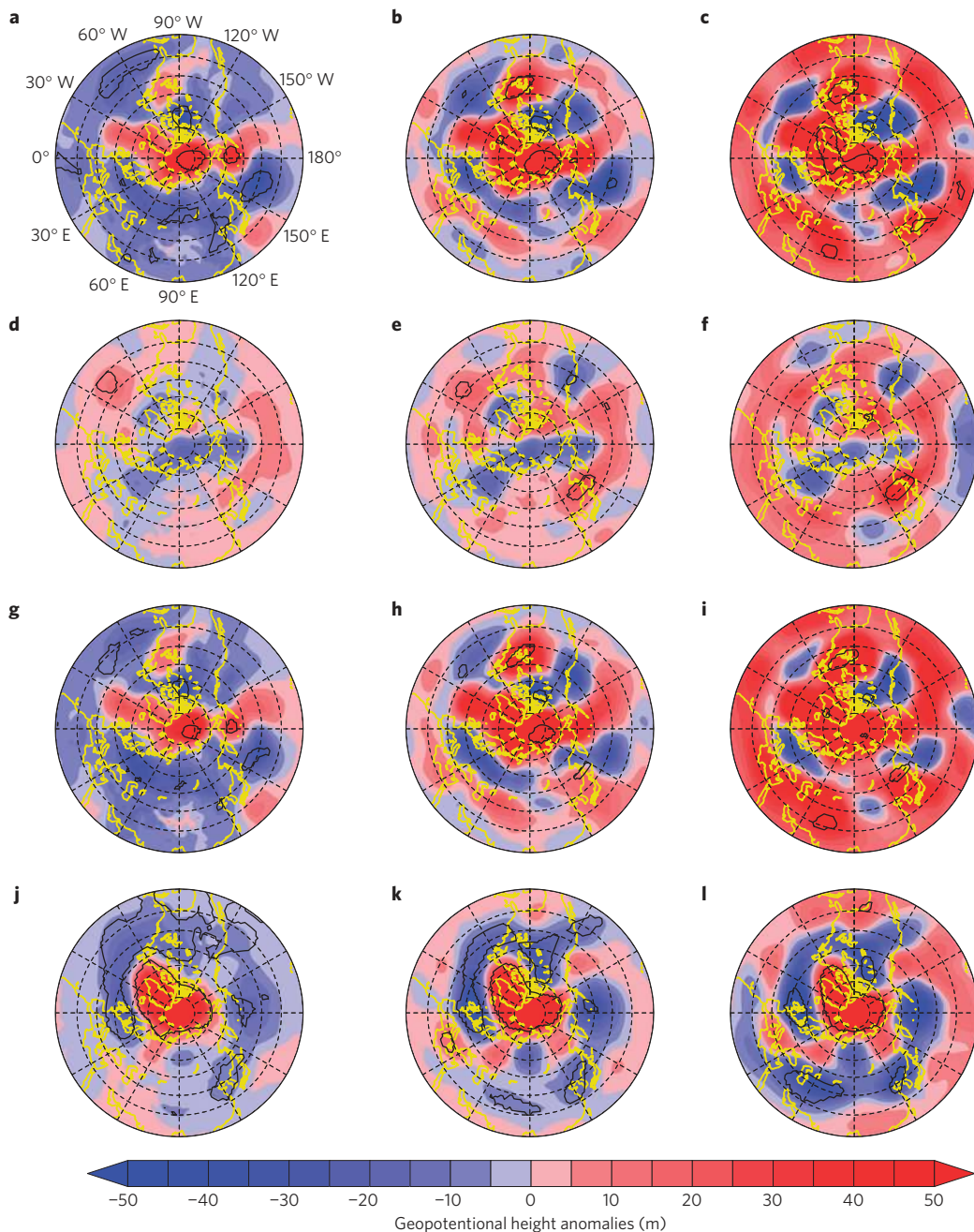
Figure 2 | Regressed height fields. a–c, Linear regression of summer (JJA) geopotential height (m) at 900 (**a**), 500 (**b**) and 200 hPa (**c**) on the detrended summer SIE index (reversed sign). **d–f**, The same as in **a–c** but for the linear regression on the detrended early summer SCE index (reversed sign). **g–i**, The same as in **a–c** but for the linear regression on the combined SIE/SCE indices. **j–l**, The same as in **a–c** but for the linear regression on the inverted Arctic Oscillation index. The regression slope gives the geopotential height anomaly that occurs in association with 1.5 million km² SIE decline (in **a–c**), 3 million km² SCE decline (in **d–f**), and the combined SIE/SCE declines (in **g–i**). The yellow outline shows the continents and regions within black contours indicate that the regression exceeds the 95% confidence level.

Arctic Oscillation index[23] shown in Fig. 1b has also become more negative in recent years, but the trend is much smaller than in SIE or SCE. The correlation between the summer Arctic Oscillation index and the third-order detrended SIE/SCE index (Fig. 1b) is small ($r = +0.14/-0.15$), accounting for only approximately 2% of the shared variances. The correlation between the detrended SIE index and SCE index is also weak ($r = +0.22$), suggesting that the interannual variabilities in the detrended SIE and SCE time series are distinct and that neither is directly related to the classic summer Arctic Oscillation, although there may be indirect

interactions between the rapidly warming Arctic and dominant modes of climate variability[24–26].

We linearly regress these three indices with geopotential heights at the 900, 500 and 200 hPa levels for JJA (Fig. 2). The responses of the atmospheric circulation to SIE and SCE anomalies are distinct. Associated with SIE loss (Fig. 2a–c), the 900 hPa anomalies (Fig. 2a) are predominantly negative over mid-latitude continents, whereas positive anomalies are evident over the North Pacific, North Atlantic and Arctic oceans. The response pattern is similar at 500 hPa (Fig. 2b), but positive anomalies are stronger and more
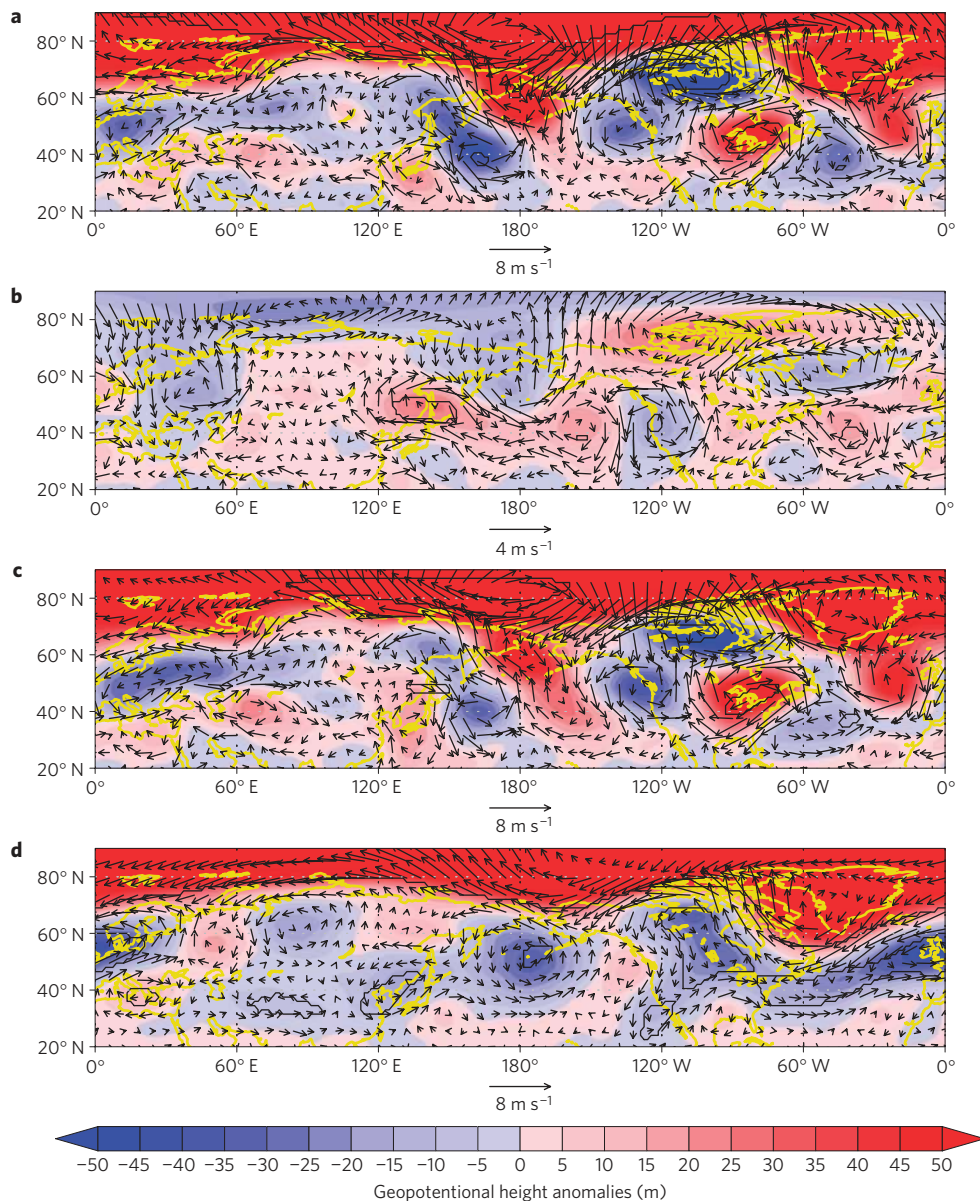
Figure 3 | Regressed wind and height anomalies. a–d, Linear regressions of the summer zonal-mean zonal and meridional wind anomalies (vectors) and geopotential height anomalies (m, colour shading) at 500 hPa on the sign-reversed detrended summer SIE index (**a**), early summer SCE index (note different vector scale; **b**), combined SIE/SCE indices (**c**), and inverted Arctic Oscillation index (**d**). The regression slope gives the geopotential height anomaly at 500 hPa that occurs in association with 1.5 million km^2 SIE decline (**a**), 3 million km^2 SCE decline (**b**), and the combined SIE/SCE declines (**c**). Black contours indicate where height anomalies exceed the 95% confidence level.

expansive, particularly over eastern North America. In some areas, such as central Asia, the sign shifts from negative to positive with height, suggesting a baroclinic response. The anomalies at 200 hPa are nearly all positive, with areas of statistically significant responses over central Asia, eastern North America, much of the Arctic and the northeastern Pacific Ocean (Fig. 2c). Areas of strong ridging with alternating negative anomalies depict a more meridional flow, suggesting slow-moving upper-level Rossby waves, consistent with expectations for the response to Arctic amplification[10]. Under these conditions, weather patterns tend to persist, increasing the probability of extreme weather events such as heat waves and drought.

Even though the area of snow-cover loss is nearly double that of sea-ice reduction, the response of the atmospheric circulation to SCE decline is much weaker (Fig. 2d–f). Associated with SCE

decline, positive anomalies are evident at the 200-hPa level over Europe, central and eastern Asia, eastern North America and the North Pacific and North Atlantic oceans (Fig. 2f). The fact that the anomalies at each level are generally collocated and increasing with height suggests that they are caused by surface heating through the snow-hydrological effect, that is, less SCE results in lower soil moisture in the summer and thus contributes to warming[11].

When height fields are regressed onto the combined SIE/SCE indices, it is clear that the sea-ice influence dominates (Fig. 2g–i). The regression patterns at all three levels are nearly identical to those in Fig. 2a–c. The prevalence of positive height anomalies suggests that in response to ice and snow loss, the subtropical semi-permanent highs may strengthen and/or shift closer to the continents[22], and thus lead to more extreme conditions, particularly over the southeastern United States[27], east Asia[4] and south Asia[28].
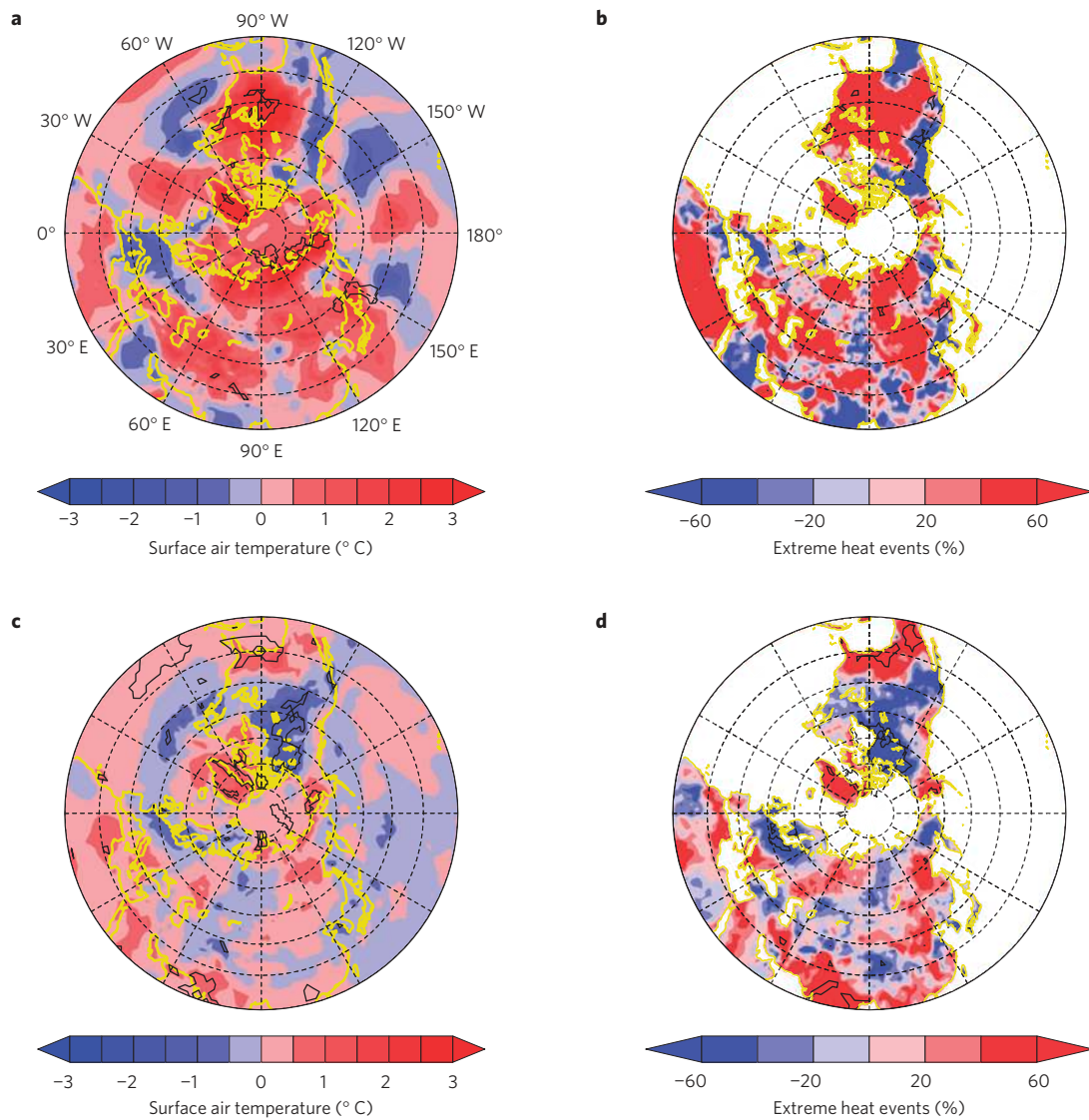
Figure 4 | Regressed surface temperature and heat events. a,b, Linear regression of surface air temperature (**a**) and extreme heat events on the detrended combined SIE/SCE indices (reversed sign; **b**). The regression slope of extreme heat events is measured as the percentage relative to the summer extreme heat event climatology during 1979–2012. **c,d**, The same as in **a,b** but regressed onto the inverted Arctic Oscillation index. Black contours indicate regions where the anomalies exceed the 95% confidence level.

The response associated with the classic Arctic Oscillation (Fig. 2j–l) is clearly different from the response to ice and snow reductions. A decreasing Arctic Oscillation index is associated with positive height anomalies over most of the Arctic along with negative anomalies around much of the mid-latitude Northern Hemisphere. These features generally persist through the atmospheric column, except over southern North America where a baroclinic structure exists.

To further elucidate the mechanisms underlying the circulation responses, we present spatial height and wind anomalies at 500 hPa regressed onto the SIE/SCE/Arctic Oscillation indices (Fig. 3). In addition to the areas of anomalous ridging described earlier, the wind field is also strongly affected by SIE reduction (Fig. 3a). Anomalous easterly flow along much of the Arctic coast is indicative of weaker upper-level zonal winds as well as a northward shift of the jet stream. This is clearly evident in the latitude/height plot of zonal-mean zonal, meridional and vertical wind anomalies (Supplementary Fig. 1a). Reduced SIE is associated with significant negative zonal wind anomalies at high latitudes,

along with enhanced meridional flow in upper levels. Increased ascending motion near 60° N and descending motion north of 80° N accompanies the wind response. The response to reduced SCE, however, is weaker (Fig. 3b), with the strongest anomalies located generally in areas where snow cover has declined. The corresponding latitude/height plot of zonal-mean wind anomalies (Supplementary Fig. 1b) corroborates this observation, as none of the zonally averaged responses is significant. In many areas the wind anomalies tend to counteract those associated with SIE losses. The combined SIE/SCE patterns of height and wind anomalies (Fig. 3c and Supplementary Fig. 1c) again illustrate the dominance of sea-ice influences on the circulation response. The spatial pattern of wind anomalies in mid-latitudes (Fig. 3c) suggests a more highly amplified flow with strong meridional anomalies across the Northern Hemisphere. The zonal upper-level winds are weaker north of 60° N, and the jet stream shifts northward in most areas. Along west coasts of continents, enhanced troughing shifts the jet stream southward and strengthens the meridional flow. These responses favour the likelihood of persistent weather

patterns that can result in increased heat waves, drought and long-lived precipitation events.

For completeness, we also present the wind and height anomalies associated with the Arctic Oscillation index (Fig. 3d and Supplementary Fig. 1d). Whereas the response in high latitudes to a negative Arctic Oscillation is similar to that for snow and ice loss, and in particular also favours strong ridging over the northwest North Atlantic and eastern North Pacific oceans, the response in mid-latitudes is distinctly different. The circulation is more zonal, with generally increasing upper-level zonal winds between 30° N and 40° N.

Finally, we present evidence of surface weather anomalies corresponding to the circulation responses. Spatial patterns of summer surface air temperature and extreme heat events are regressed onto the combined SIE/SCE and the Arctic Oscillation indices (Fig. 4). The summer temperature response associated with SIE/SCE reduction reveals predominantly positive temperature anomalies spanning the northern continental areas (Fig. 4a), with extreme heat events occurring over the eastern half of North America, eastern Europe and eastern Asia (Fig. 4b). Negative temperature anomalies are located along the continental west coasts, where upstream anomalous ridging over the extratropical oceans favours incursions of cool and wet air masses from the ocean[5]. These anomalies are not statistically significant, however. A negative Arctic Oscillation index is associated with positive temperature anomalies (Fig. 4c) and extreme heat events along southern North America and southern Asia (Fig. 4d). These locations are related to the descending motion in lower latitudes associated with a negative Arctic Oscillation phase (Supplementary Fig. 1d).

The results of this study demonstrate linkages between losses of snow and ice in the Arctic and summer weather patterns in mid-latitudes. On the basis of regression analyses of summer sea-ice and early summer snow-cover anomalies with atmospheric features, we find the following:

First, circulation responses to ice loss, snow loss and the Arctic Oscillation phase are distinct.

Second, even though the area of snow loss during May/June is approximately twice the area of summer sea-ice loss, the response to sea-ice loss is significantly stronger. A likely reason is that the contrast in reflectivity between ice and open ocean is much larger than that between snow and the underlying surface, particularly in areas covered with shrubs and trees.

Third, anomalies in summer geopotential heights associated with ice and snow loss increase with height.

Fourth, the response to SCE loss favours descending air motion in mid-latitudes, which contributes to positive temperature anomalies and increased extreme heat events over mid-latitude continents.

Fifth, the response to the combined SIC/SCE loss suggests that the zonal jet-stream winds are weakened and the jet is shifted northward. The large-scale waves are amplified, which tends to favour more persistent weather systems and a higher likelihood of summer weather extremes.

Although there is much still to learn about the interactions between a rapidly changing Arctic and large-scale circulation patterns, this study builds on earlier work and provides further evidence linking snow and ice loss in the Arctic with summer extreme weather in mid-latitudes. As greenhouse gases continue to accumulate in the atmosphere and all forms of Arctic ice continue to disappear, we expect to see further increases in summer heat extremes in the major population centres across much of North America and Eurasia where billions of people will be affected.

Methods

Summer (JJA) surface air temperature, geopotential heights, and winds (monthly fields) were obtained from the latest reanalysis of the European Centre for Medium-Range Weather Forecasts (ERA-Interim, 1979–2012; ref. 14). Arctic SIE (that is, area with at least 15% sea-ice cover) derived from passive microwave satellite observations using data from the Nimbus 7 Scanning Multichannel Microwave Radiometer and three Defense Meteorological Satellite Program Special Sensor Microwave Imager sensors[13] were obtained from the National Snow and Ice Data Center (http://nsidc.org/data/seaice_index/). The SCE data were obtained from the Global Snow Lab at Rutgers University (http://climate.rutgers.edu/snowcover/), and the monthly Arctic Oscillation index was defined as the principal component time series of the first leading mode of rotated empirical orthogonal function analysis of the monthly mean 500-mb height over the Northern Hemisphere from the National Oceanic and Atmospheric Administration Climate Prediction Center (http://www.cpc.noaa.gov/). Extreme heat events are defined as the days when ERA-Interim daily maximum surface air temperature exceeded a specified threshold corresponding to 1.5 standard deviations above the local climatological daily mean in 1979–2012 (refs 12,23).

An optimal polynomial trend line, the order of which suggested by the leave-one-out cross-validation method was three[29], was used to fit the long-term change in summer Arctic SIE and early summer Northern Hemisphere SCE (refs 12,30). The binary linear regressions of summer fields on the third-order detrended summer SIE and early summer SCE indices during 1979–2012 were computed. The regression onto the combined SIE/SCE indices, that is, the sum of 1.5 times the regression slope of SIE and 3 times the regression slope of SCE (with units of million square kilometres), is shown. The regression onto the combined SIE/SCE indices thus represents the anomaly in a variable that occurred in association with a 1.5 million km² decline in Arctic SIE and a 3 million km² decline in SCE. The regression slopes of extreme heat events are further divided by their respective mean values in 1979–2012 to obtain percentage anomalies in association with a 1.5 million km² decline in Arctic SIE and a 3 million km² decline in SCE.

References

1. Peterson, T. C., Hoerling, M. P., Stott, P. A. & Herring, S. C. (eds) Explaining extreme events of 2012 from a climate perspective. *Bull. Am. Meteorol. Soc.* **94,** S1–S74 (2013).
2. Coumou, D. & Rahmstorf, S. A decade of weather extremes. *Nature Clim. Change* **2,** 491–496 (2012).
3. Sutton, R. T. & Dong, B. Atlantic Ocean influence on a shift in European climate in the 1990s. *Nature Geosci.* **5,** 788–792 (2012).
4. Seo, K-H., Son, J-H., Lee, S-E., Tomita, T. & Park, H-S. Mechanisms of an extraordinary East Asian summer monsoon event in July 2011. *Geophys. Res. Lett.* **39,** L05704 (2012).
5. Comiso, J. C. Large decadal decline of the Arctic multiyear ice cover. *J. Clim.* **25,** 1176–1193 (2012).
6. Stroeve, J. C. et al. The Arctic's rapidly shrinking sea ice cover: a research synthesis. *Climatic Change* **110,** 1005–1027 (2012).
7. Derksen, C. & Brown, R. Spring snow cover extent reductions in the 2008–2012 period exceeding climate model projections. *Geophys. Res. Lett.* **39,** L19504 (2012).
8. Jaeger, E. B. & Seneviratne, S. I. Impact of soil moisture–atmosphere coupling on European climate extremes and trends in a regional climate model. *Clim. Dynam.* **36,** 1919–1939 (2011).
9. Overland, J. E., Francis, J. A., Hanna, E. & Wang, M. The recent shift in early summer Arctic atmospheric circulation. *Geophys. Res. Lett.* **39,** L19804 (2012).
10. Francis, J. A. & Vavrus, S. J. Evidence linking Arctic amplification to extreme weather in mid-latitudes. *Geophys. Res. Lett.* **39,** L06801 (2012).
11. Matsumura, S. & Yamazaki, K. Eurasian subarctic summer climate in response to anomalous snow cover. *J. Clim.* **25,** 1305–1317 (2012).
12. Tang, Q., Zhang, X., Yang, X. & Francis, J. A. Cold winter extremes in northern continents linked to Arctic sea ice loss. *Environ. Res. Lett.* **8,** 014036 (2013).
13. Cavalieri, D. J. & Parkinson, C. L. Arctic sea ice variability and trends, 1979–2010. *Cryosphere* **6,** 881–889 (2012).
14. Dee, D. P. et al. The ERA-Interim reanalysis: configuration and performance of the data assimilation system. *Q. J. R. Meteorol. Soc.* **137,** 553–597 (2011).
15. Polyakov, I. V. et al. Observationally based assessment of polar amplification of global warming. *Geophys. Res. Lett.* **29,** 1878 (2002).
16. Screen, J. A., Deser, C. & Simmonds, I. Local and remote controls on observed Arctic warming. *Geophys. Res. Lett.* **39,** L10709 (2012).
17. Serreze, M. C. & Francis, J. A. The Arctic amplification debate. *Climatic Change* **76,** 241–264 (2006).
18. Screen, J. A. & Simmonds, I. The central role of diminishing sea ice in recent Arctic temperature amplification. *Nature* **464,** 1334–1337 (2010).
19. Porter, D. F., Cassano, J. J. & Serreze, M. C. Local and large-scale atmospheric responses to reduced Arctic sea ice and ocean warming in the WRF model. *J. Geophys. Res.* **117,** D11115 (2012).
20. Liu, J., Curry, J. A., Wang, H., Song, M. & Horton, R. M. Impact of declining Arctic sea ice on winter snowfall. *Proc. Natl Acad. Sci. USA* **109,** 4074–4079 (2012).

21. Petoukhov, V., Rahmstorf, S., Petri, S. & Schellnhuber, H. J. Quasiresonant amplification of planetary waves and recent northern hemisphere weather extremes. *Proc. Natl Acad. Sci. USA* **110,** 5336–5341 (2013).
22. Li, W., Li, L., Ting, M. & Liu, Y. Intensification of Northern Hemisphere subtropical highs in a warming climate. *Nature Geosci.* **5,** 830–834 (2012).
23. Thompson, D. W. J. & Wallace, J. M. The Arctic Oscillation signature in the wintertime geopotential height and temperature fields. *Geophys. Res. Lett.* **25,** 1297–1300 (1998).
24. Stroeve, J. C. *et al.* Sea ice response to an extreme negative phase of the Arctic Oscillation during winter 2009/2010. *Geophys. Res. Lett.* **38,** L02502 (2011).
25. Ogi, M. & Wallace, J. M. The role of summer surface wind anomalies in the summer Arctic sea ice extent in 2010 and 2011. *Geophys. Res. Lett.* **39,** L09704 (2012).
26. Jaiser, R, Dethloff, K. & Handorf, D. Stratospheric response to Arctic sea ice retreat and associated planetary wave propagation changes. *Tellus A* **65,** 1–11 (2013).
27. Li, W., Li, L., Fu, R., Deng, Y. & Wang, H. Changes to the North Atlantic subtropical high and its role in the intensification of summer rainfall variability in the southeastern United States. *J. Clim.* **24,** 1499–1506 (2011).
28. Lau, W. K. M. & Kim, K-M. The 2010 Pakistan flood and Russian heat wave: teleconnection of hydrometeorological extremes. *J. Hydrometeorol.* **13,** 392–403 (2012).
29. Weisberg, S. *Applied Linear Regression* 3rd edn (Wiley, 2005).
30. Eisenman, I. Geographic muting of changes in the Arctic sea ice cover. *Geophys. Res. Lett.* **37,** L16501 (2010).

Author contributions

Q.T. and J.A.F. designed the study. Q.T., X.Z. and J.A.F. conducted the analysis and all of the authors contributed to the paper writing.

Additional information

Supplementary information is available in the online version of the paper. Reprints and permissions information is available online at www.nature.com/reprints. Correspondence and requests for materials should be addressed to Q.T.

Competing financial interests

The authors declare no competing financial interests.